

# Three-phase Control for Miniaturization of a Snake-like Swimming Robot

Jonathan Rossiter<sup>\*†</sup>, Boyko Stoimenov<sup>†</sup>, Yoshihiro Nakabo<sup>‡</sup>, Toshiharu Mukai<sup>†</sup>

<sup>\*</sup>Dept. of Engineering Mathematics,  
University of Bristol  
Bristol,  
BS8 1TR, UK

<sup>‡</sup>Safety Intelligence Research Group,  
Intelligent Systems Institute,  
National Institute of Advanced Industrial  
Science and Technology (AIST),  
1-1-1, Tsukuba, 305-8568, JAPAN

<sup>†</sup>Bio-mimetic Control Research Center,  
RIKEN (The Institute of Physical and  
Chemical Research),  
2271-130, Moriyama-ku, Nagoya,  
463-0003 JAPAN

Jonathan.Rossiter@bris.ac.uk

nakabo-yoshihiro@aist.go.jp

{Rossiter, Stoimenov, Tosh}@bmc.riken.jp

**Abstract** – We present the design and control of a soft undulating snake-like swimming robot that can be miniaturized down to the millimeter scale. We consider the miniaturization of an ionic polymer metal composite (IPMC) robot with respect to Reynolds number and propose biologically inspired undulating motion as a suitable swimming mechanism that can scaled down in excess of three orders of magnitude. We examine the control system needed to generate this undulating motion and take inspiration from poly-phase electrical power delivery systems to greatly simplify the control system, while maintaining the ability to move forwards and backwards and to turn. As a result of the simplified three-phase control we can further simplify the structure of the robot and make miniaturization more practical.

**Index Terms** – IPMC, anguilliform, snake-like, swimming robot.

## I. INTRODUCTION

In this paper we present a six-segment soft swimming robot made from bending actuator material, such as ionic polymer metal composite (IPMC.) Previously we have presented a 7-segment snake-like swimming robot made from IPMC material that was 140mm long [3][4]. Our goal now is to design a simple robot body and control mechanism that can easily be miniaturized to make the next generation micro swimming robots. We expect scaled versions of this robot, with length ranging from about 20cm to less than 5mm, to swim using the same design.

As a swimming mechanism we take inspiration from animals, such as anguilliforms, swimming snakes, and other BCF (Body and/or Caudal Fin) locomotors [1][2]. These animals move by undulating segments of their bodies in a side-to-side movement. Forward thrust is generated by the inertial and viscous forces of the liquid medium as a traveling wave propagates from head to tail.

There are a number of problems in miniaturizing such a swimming robot. Firstly we must consider the scalability of the swimming mechanism given the properties of the liquid. As we will propose in the next section, the undulating-type swimming motion is a suitable scalable motion. Secondly we need to consider the scalability of the body. Here the material properties of film metal-polymer bending actuators are ideal. Finally we need to consider the scalability of the control mechanism, especially with respect to complexity and power handling.

In the next section we argue for undulating swimming motion by examining the Reynolds number of the scaled robot at different scales. In the sequel we discuss practical aspects of miniaturization and present a number of important design improvements and simplifications to the robot body and the control system.

## II. MOTIVATION FOR SIMPLE UNDULATORY MOTION

The animal kingdom has evolved many different mechanisms for propulsion in water. The large variety of mechanisms is a result of the different characteristics of water at different scales [1]. We can characterize the type of motive mechanism around the Reynolds number,  $Re$ , itself dependent on liquid properties and the size and velocity of the moving animal [2]:

$$Re = \frac{v_s L}{\nu} \quad (1)$$

where  $L$  is the characteristic length,  $v_s$  is the velocity of the animal, and  $\nu$  is the kinematic viscosity of the liquid ( $1 \times 10^{-6} \text{m}^2 \text{s}^{-1}$  for water at  $20^\circ \text{C}$ ).

For high Reynolds numbers swimming animals rely on inertia forces. At low Reynolds number inertia forces become insignificant and viscosity forces dominate.

In this paper we consider a swimming robot that can be scaled from approximately 20cm down to a size where it can, for example, swim through large blood vessels. As such we need to consider Reynolds numbers of both the largest robot (say 20cm) and the smallest robot (say 5mm). Consider a swimming robot made from a single bending actuator sheet with dimensions 20cm\*3cm which travels at 10cm/s in water. The Reynolds number will be 20000, a number at which both viscous and inertial forces operate. Now we scale this down to fit an application such as swimming in small fluid-filled pipes. We linearly shrink the above robot to dimensions of 5mm\*0.75mm and assume it travels at 2.5mm/s in water. The Reynolds number will now be 12.5. Further, in [1] it is suggested that it is often more useful to consider the Reynolds number for side-to-side movement rather than length-wise movement. In this case we might consider the width of the robot (0.75mm) as the closest equivalent to the diameter of an undulating tube. Now assuming the undulations have speed of, say, 5mm/s in water we calculate a Reynolds number of

3.75. If the same robot swims in blood the Reynolds number will be further reduced by a factor of approximately 4.

The approximate range for the Reynolds number for our scalable swimming robot is conservatively taken to be approximately 0.1 to 20000. Of course, for smaller robots this range will extend to even smaller Reynolds numbers. Fig. 1. shows Reynolds number and the balance of inertial and viscous forces [7]. Region A shows the approximate range of Reynolds number we are considering in this paper.

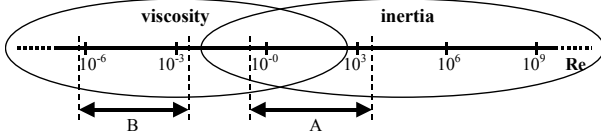


Fig. 1 Reynolds number and dominant forces

A swimming mechanism that seems to cover this whole range is that which involves bending along the body to create a head-to-tail traveling wave. Anguilliforms (such as eels) using undulating motion have Reynolds numbers towards the upper end of region A (calculated from data in [6]). The movements of anguilliforms are also quite similar to the patterns shown by bacteria and protozoa using resistive propulsion ([5]) at low Reynolds numbers ( $10^{-6} - 10^{-3}$ ) shown as region B in Fig. 1. We therefore adopt such undulation motion as a suitable scalable motion.

Further to this we may revisit the results in [3] which show increased amplitudes of bending towards the tail of a 140mm long, 7-segment snake-like swimming robot, despite each segment being driven by signals with the same amplitude. The higher Reynolds number in this case means a higher component of inertia forces and these forces may contribute to the exaggerated bending in the tail sections. The phenomenon of increasing transverse movements from head to tail naturally occurs in undulating fish, including anguilliforms where almost all of the body undulates. The previous 7-segment robot is a good demonstration of anguilliform motion (with increasing amplitude towards the tail) generated by uniform harmonic excitation along the robot. We would expect such an excitation mechanism to generate a more uniform movement in smaller robots where the Reynolds number is lower.

The above discussion suggests that, in order to design a swimming robot that can motivate at a wide range of scales (approximately three orders of magnitude in size and approximately five orders of magnitude in terms of Reynolds number) simple undulatory motion is suitable. Not only that, but the proposed uniform body shape further mimics the shape of smaller undulatory swimmers, such as the nematode worm [5], and is expected to promote efficient movement at smaller scales.

### III. A SIX-SEGMENT IPMC SWIMMING ROBOT

It is common for many undulatory swimmers from large anguilliforms (e.g. eel or lamprey) to small protozoa (e.g. nematode) to have a body length the same as, or longer than,

the wavelength of the head-to-tail traveling wave. We thus propose a swimming robot with body length (minus the head containing the controller) equal to the wavelength of the traveling wave. In [4] we presented a 7 segment snake-like robot where each successive segment was driven by a sine wave with additional phase difference of  $\pi/3$ . Thus the robot length covered  $7/6$  of the wavelength  $\lambda$  of the driving signal. We propose to use the same  $\pi/3$  out-of-phase signals for successive segments but restrict the length of the robot to six segments and thus one wavelength. The proposed robot is shown in Fig. 2. The reason for choosing a multiple of 3 for the number of segments is important and is discussed in the next section.

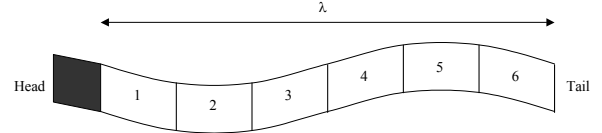


Fig. 2 The six-segment swimming robot

### IV. THREE-PHASE CONTROL OF SIX-SEGMENT ROBOT

Given six segments ( $N=6$ ) and a  $\pi/3$  phase difference the driving signals to each segment will be:

$$E_n = \sin(x - (n-1)\pi/3) \quad n \in \{1, \dots, N\} \quad (2)$$

In previous snake-like swimming robots we have generated  $N$  independent signals and delivered them to the  $N$  segments by pairs of conductors. Clearly this requires  $2N$  conductors in total. In this paper we take inspiration from electrical supply systems and deliver power to the 6-segment snake using a balanced poly-phase configuration.

Consider the conventional three-phase star (or “wye”) connected sources shown in Fig. 3.

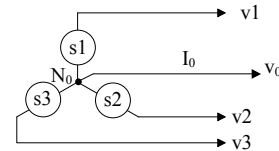


Fig. 3 Three-phase source connections

Here the three sources  $\{s1, s2, s3\}$  generate three sine waves (or phases),  $\{v1, v2, v3\}$ , each  $2\pi/3$  out of phase. I.e.

$$v_n = \sin(x - (n-1)2\pi/3) \quad n \in \{1, \dots, 3\} \quad (3)$$

When delivering power to a load, any phase imbalance will result in a neutral current  $I_0$  flowing. If, on the other hand, we can guarantee a balanced load then neutral current  $I_0$  will be zero and this connector can be removed. The robot segments also need to be configured for three-phase control. The two possible load configurations are shown in Fig. 4.

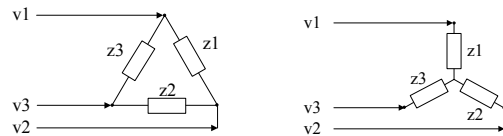


Fig. 4 Three-phase balanced load connections, delta (left) and star (right)

The two configurations in Fig. 4 each have their own advantages and disadvantages. The biggest difference in this

context is that the amplitude of the voltage sine waves across the loads  $\{z_1, z_2, z_3\}$  in the delta configuration are  $\sqrt{3}$  times the amplitude of the source voltages  $\{v_1, v_2, v_3\}$ . In the star connected load the voltage signals across the loads are the same as the source voltage signals.

Using such a balanced three-phase source as described above we can supply three of the sine waves defined in (2) using only three connectors (e.g.  $E_1=v_1$ ,  $E_3=v_2$  and  $E_5=v_3$  for star connected load.) Thus we have reduced the number of conductors by half.

We can further simplify the poly-phase control and delivery of power to the six segments by utilizing the polarity of the robot segments. That is, a positive voltage across a segment results in bending in one direction and a reverse voltage results in bending in the opposite direction. Taking this into account we can see that driving signals  $E_2$ ,  $E_4$ , and  $E_6$  can be derived from  $E_1$ ,  $E_3$  and  $E_5$ . In other words:

$$\begin{aligned} E_2 &= \sin(x - \pi/3) = -\sin(x - 4\pi/3) = -E_5 \\ E_4 &= \sin(x - \pi) = -\sin(x) = -E_1 \\ E_6 &= \sin(x - 5\pi/3) = -\sin(x - 2\pi/3) = -E_3 \end{aligned} \quad (3)$$

We can now connect all six robot segments as polarized components to a single three-phase source as shown in Fig. 5. Note that bands on the loads show polarity with respect to the sides of the robots snake body.

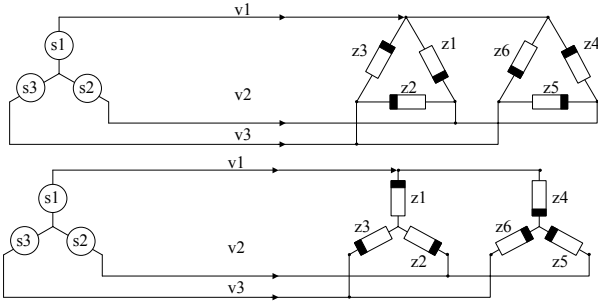


Fig. 5 Three-phase balanced load connections for six polarized segments, delta (top) and star (bottom)

Using such a configuration it is clear that six distinct  $\pi/3$  out-of-phase sine waves can be delivered to six segments using only three sources and three conductors. This offers a great saving in size of components, complexity of control circuit and amount of wiring. The six sine waves generated from the single 3-phase source are shown in Fig 6.

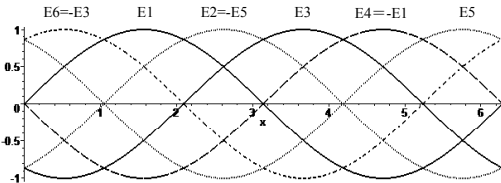


Fig. 6 Six driving signals generated from polarized 3-phase connections

#### IV. CONNECTIONS TO THE ROBOT BODY

Now let us consider the body of the 6-segment snake-like robot. Using a system of 6 separate sources (as in [4]) we would need to connect the six segments as shown in Fig. 7 using 12 conductors. If on the other hand we use only a three-

phase supply and connect the segments in a polarized delta confirmation as in Fig. 5 we obtain the greatly simplified connections in Fig. 8. Likewise, if we connect the segments in a polarized star configuration we obtain the connections in Fig. 9. Note again that in both these configurations only three signal sources and only three conductors are used.

In Fig. 9 it is clear that three segments on either side of the robot are connected together but isolated from the supplies. These segment connections correspond to the neutral point  $N_0$  in Fig 3. Since we assume the power delivered to each segment is the same, and thus the three-phase loads are balanced, no connection is needed from these isolated segments to the  $N_0$  point.

Another, more important, observation is that in the delta connected configuration of Fig. 8 there are 5 pairs of adjacent segment electrodes that are connected together (three pairs on side 2 and two pairs on side 1.) Since these connections carry the same signal we can merge the respective electrodes on each side to give the simplified robot body shown in Fig 9. Now we have only two segmentation boundaries on one side and three on the other. This further simplified the structure of the robot. Not only that, but segmentation boundaries are points where mechanical stress is introduced into the structure (e.g. through machining or laser cutting of the electrodes) and we would naturally want to reduce their number.

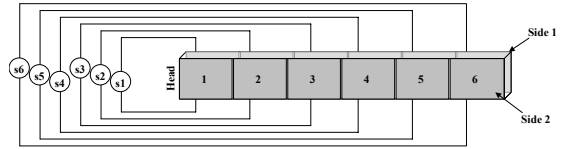


Fig. 7 segment connections using separate sources

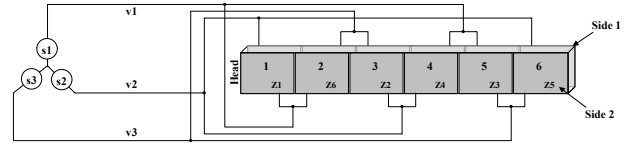


Fig. 8 segment connections using delta configuration

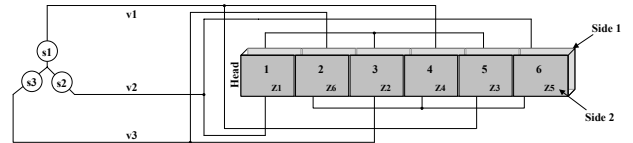


Fig. 9 segment connections using star configuration

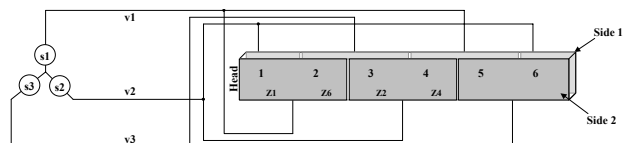


Fig. 10 delta connected segments further simplified

#### V. CONTROL SIGNALS

While it should be clear that forward motion of the 6-segment, 3-phase connected snake simply involves operating the 3-phase sources in the normal continuous mode, some thought must be given to how other motions can be achieved. For

example, in [4] we showed that the previous 7-segment snake was able to move forward and backwards and also to turn left and right. How can we achieve these motions given the inherent restrictions of a single 3-phase supply?

#### A. Reverse motion

Swimming in reverse is simply a case of reversing the order of the signals in the 3-phase sources:

$$v_n = \sin(x + (n-1)2\pi/3) \quad n \in \{1, \dots, 3\} \quad (3)$$

This gives reverse movement identical to that shown in [4] but again, only requires the 3-phase signals.

#### B. Left and right turning

Where straight forward motion in anguilliforms involves all body sections bending with constant amplitude, turning left and right involves controlled changes to the amplitude of bending in appropriate segments [8]. In this way a difference in thrust is generated between the two sides of the fish and it turns. Such an activation function for one segment might resemble Fig. 11 where amplitude decreases in the second half wavelength.

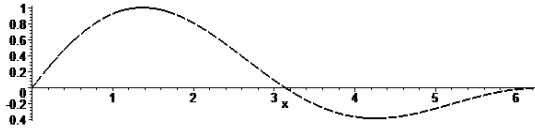


Fig. 11 Possible segment activation function for anguilliform-like turning

Unfortunately this form of unbalanced bending activation is incompatible with IPMC actuators. This is a consequence of the capacitance-like characteristic of the IPMC [9]. Activation of the IPMC involves charging a large capacitance component. An activation signal such as that shown in Fig. 11 has an integral over one wavelength that is non-zero. Such a non-zero integral will result in gradual DC charging of the IPMC capacitance. A DC biased IPMC will respond poorly to a subsequent AC bending signal.

Thus we need to generate driving signals for the IPMC that integrate to zero. One solution presented in [4] is to change the speed of the activation signal within one wavelength. Such an activation signal is shown in Fig. 12 and was shown to produce sideways turning motion.

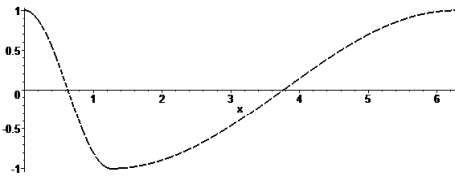


Fig. 12 Activation function for turning motion

Unfortunately such a signal is not readily achievable with delta-connected 3-phase loads. This is because, in the delta-connected load, the voltage across each load element is the difference between two source signals. We seek therefore to generate a close approximation to the function in Fig. 12 across the loads, rather than at the sources. Fig. 13 shows

modified 3-phase source signals, one phase of which can be defined over a single period by:

$$v = \begin{cases} \sin((p-x)^2) & : x < p \\ \sin((x-p)^2) & : x \geq p \end{cases} \quad (6)$$

where  $p = (\pi/2)^{1/2}$ . These source signals generate asymmetric load signals, one of which is shown in Fig. 14. Note the greater rate of change in amplitude in the first third of the signal.

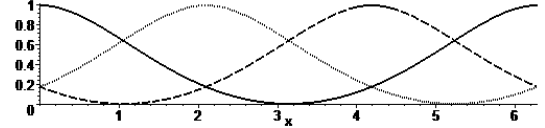


Fig. 13 3-phase source signals for turning motion

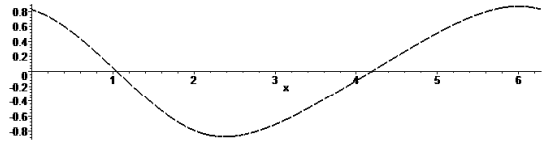


Fig. 14 3-phase load signals for turning motion

We can further exaggerate this effect at the expense of smoothness by increasing the order of the function:

$$v = \begin{cases} \sin((p-x)^4) & : x < p \\ \sin((x-p)^4) & : x \geq p \end{cases} \quad (7)$$

where  $p = (\pi/2)^{1/4}$ . These source signals are shown in Fig. 15 and generate exaggerated load signals as shown in Fig. 16, which is a reasonable approximation to Fig. 12.

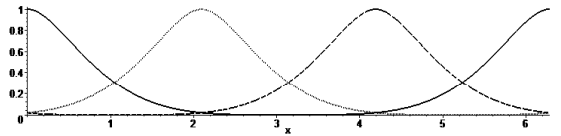


Fig. 15 3-phase exaggerated source signals for turning motion

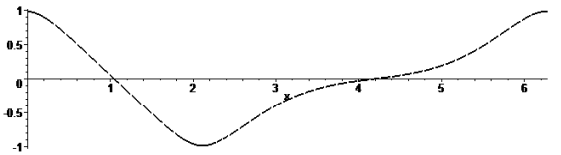


Fig. 16 3-phase exaggerated load signals for turning motion

It is important to note here that we are restricted by the 3-phase sources such that the fastest maximum-to-minimum smooth transition within these turning signals occupies no less than  $2\pi/3$  of the wavelength, the phase difference between the 3-phase signals.

## VI. ELECTRICAL CONTROL SYSTEM

Next we consider the electrical control system required by an autonomous six-segment swimming robot of this type. There are many ways to electrically control IPMC actuators but we can generally class these into either analog drivers or digital switching drivers. An analog driver will deliver a varying analog voltage to the actuator that will bend more with increasing voltage. Digital switching drivers typically use a pulse width modulation (PWM) control signal and a constant

voltage supply to deliver discretely varying power that is smoothed either in the load device itself or in external components. Analog driver circuits are more complicated but can enable greater precision when connected to reactive components. Digital switching circuits are often much smaller and easier to implement but extra considerations need to be taken into account, especially concerning the reactive components of the load and the frequency of digital switching.

*A. Motion from a 3-phase analog driver*

In [4] we controlled the 7-segment snake-like robot using a personal computer and seven analog output amplifiers. As a test of the 3-phase source model presented in this paper we connected the 7-segment robot to a 3-phase analog source (by using only three of the analog output amplifiers) as shown in Fig. 7, where the 7<sup>th</sup> segment was connected in the same fashion as the first segment. Forward and backward movement of the 3-phase robot exactly matched the movement of the same device when driven by the seven separate signals. This was achieved even given the imbalanced load (7 segments instead of 6.) This demonstrates the feasibility of 3-phase analog drive for such a snake-like swimming robot.

*B. Motion from a 3-phase digital switching driver*

Next we designed and implemented the very simplest digital half-bridge switching circuit that can be driven by one digital signal. The circuit is shown in Fig. 17a, where resistor Ra and Rb values were chosen to ensure the transistors only turn on when the input has clear logic 1 or 0. Three of these circuits, DC1 - DC3, were connected to three pins of a microcontroller (dsPIC,) as shown in Fig. 17b, and were driven by PWM signals to generate the three 3-phase signals. Note that these switching drivers will generate analog voltages in the range [0,+Vs] but when applied to delta-connected loads will deliver load voltages in the range [-Vs,+Vs].

Thus we have a full 3-phase control circuit comprising 6 transistors, 12 resistors and a small microcontroller. Given micro-sized components and modern fabrication techniques it is entirely feasible to make the whole circuit small enough to fit on the head of our smallest intended swimming robot (5mm in length.)

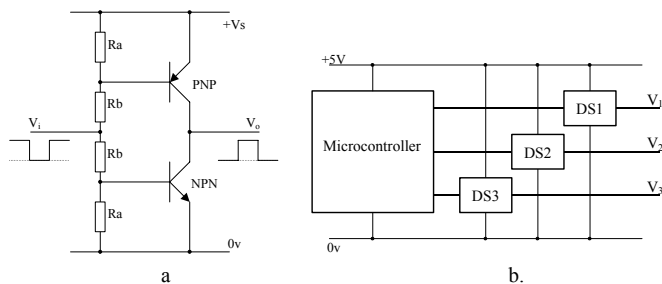


Fig. 17 switching and control circuit to deliver 3-phase signals

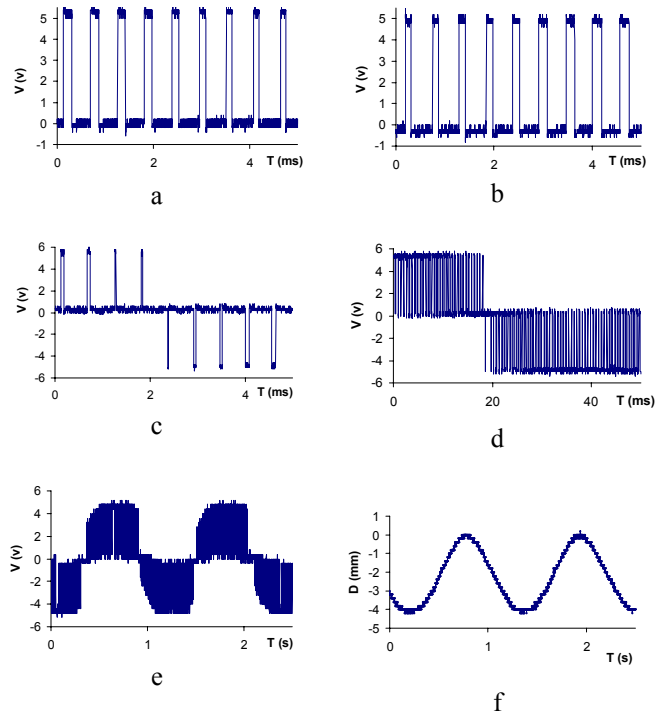


Fig. 18 PWM signals across an IPMC actuator

Now let us consider the PWM signals as they are applied to an IPMC load. Fig. 18 shows experimental data recorded when driving one IPMC segment using the above digital switching driver. Fig. 18a and 18b show two of PWM output signals with no load connected. These two signals define the first two phases of the 3-phase source. Fig. 18c shows the difference between these signals and it clearly shows the point where the digitised sine wave crosses the 0v axis. Fig. 18d shows the same signal as 18c but over a longer time period. This is the signal that is applied to a single segment in the IPMC snake-like robot. Fig. 18e shows the voltage across the load segment driven by the unfiltered PWM signal in 18d. Note how there is some natural filtering action but that the high frequency digital PWM component remains very much in evidence. More importantly from the point of view of swimming motion, Fig. 18f shows the displacement of the activated segment as recorded by a Keyence laser displacement meter. Fig. 18f shows a clear and smooth sine wave of the same frequency and phase as the PWM encoded sine wave delivered to the load (Fig. 18e.) Note that quantisation in these plots is an artefact of the sampling oscilloscope used to record this data.

We can draw several conclusions from this data:

- A digital switching 3-phase driver generates a clean and smooth sine wave for segment displacement.
- There is an element of natural filtering in the IPMC that smooths out some of the PWM signal.
- The large equivalent capacitance in the IPMC material acts as a differentiator circuit thus limiting effective smoothing.

- Even though the voltage signal suggests that the power delivery is not optimal, the simplicity of the driver and the smooth actuation of the segment mean that it has real practical application in miniature snake-like robots.

### C. More efficient power delivery into an IPMC load

The large capacitance model of the IPMC has consequences for PWM driving of the 6-segment snake. Every time the PWM signal changes state it results in a switch in transistor in the circuit in Fig. 17. For a perfect capacitance, with zero resistive component, this would result in the full supply voltage being applied instantaneously across the “on” transistor. For a typical transistor with small emitter-collector “on” resistance this voltage would result in a large instantaneous current flowing. Possible consequences of this include burnout of the transistor, burnout of current carrying conductors, burnout of portions of the metal electrode on the IPMC and a loss in efficiency in power delivery.

To circumvent this we may limit the maximum current that flows into the IPMC (i.e. the equivalent capacitance.) This can be achieved by adding a resistive component in series with the load, but this will result in an  $I^2R$  resistive power loss. An alternative is to use a constant current source instead of a voltage source and switch this current source using the PWM signal. This is more efficient with respect to delivery of power to the load, but the source will be much more complex than the voltage source (which may simply be a battery cell) and efficiency of the source itself may not be great.

A better alternative is a simple circuit that actively switches the voltage supply but also reduces maximum current. Such a circuit may be realized using a simple and compact dc-dc converter such as the Buck converter shown in Fig. 19. In such a circuit the PWM signal is typically used to control the voltage across a resistive load. When driving a capacitive load the Buck converter can be used to limit maximum current through the circuit and also the amount of energy transferred per switching cycle. Additionally, for additional versatility, the Buck converter circuit can be controlled by varying the frequency of a constant duty cycle switching signal. A further benefit is the high efficiency of this circuit, which is expected to surpass the efficiency of the alternatives described above.

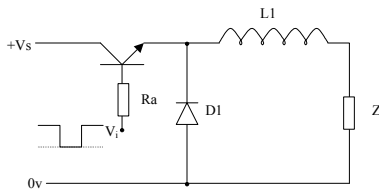


Fig. 19 Buck converter

In practice though, we have found no great problem in driving the 6-segment swimming robot using the simple voltage switched PWM circuit in Fig. 17. From our measurements we have found that the impedance of the IPMC

contains a measurable series resistance component of about 5 ohms (for a 40mm by 4mm sample) and for the largest 6-segment and 7-segment swimming robots the switching transistors switch maximum instantaneous currents in the region of 1amp without excess heating.

## VI. CONCLUSIONS

Autonomous miniature swimming robots have a high potential for medical applications, such as analysis of blood vessel condition. We have shown that many of the features required for the realization of such miniature robots are already present in a snake-like swimming robot that we have previously developed. Snake-like undulatory motion is well suited to miniaturization and is expected to work well under the low Reynolds numbers resulting from the smaller size. The body of the snake, which is made of soft IPMC actuator material, is easily scalable down to the millimeter scale.

In this paper we also present a solution to the serious problem in miniaturization resulting from the need for individual control of each section along the length of the snake. We have replaced individual section control by a simpler three-phase control of six segments connected in a star- or delta-shape and we demonstrated the feasibility of this approach. We have also demonstrated the feasibility of pulse width modulation (PWM) control of the miniaturized device. Implementing the hardware control circuit would be the next step to a miniature snake-like swimming robot.

## ACKNOWLEDGMENTS

Dr Jonathan Rossiter is currently the holder of a Royal Society Research Fellowship and this research has been made possible by the generous support of the Royal Society.

## REFERENCES

- [1] R. McNeill Alexander, *Principles of Animal Location*, Princeton Uni. Press, 2003.
- [2] A. A. Biewener, *Animal Location*, Oxford Uni. Press, 2003.
- [3] Y. Nakabo, K. Takagi, T. Mukai, Z. Luo, K. Asaka, “Snake-like Swimming Artificial Muscle -A Bio-Mimetic Soft Robot,” Proc. of Third Conference on Artificial Muscles, May 30-31, 2006, Tokyo.
- [4] Y. Nakabo, T. Mukai, Asaka, “Propulsion model of snake-like swimming artificial muscles,” Proc. of IEEE International Conference on Robotics and Biomimetics, June 29-July 03, 2005, Hong Kong.
- [5] J. Bryden, N Cohen, “A simulation model of the locomotion controllers for the nematode *caenorhabditis elegans*,” The Eighth International Conference on the Simulation of Adaptive Behavior (SAB’04) 13 - 17 July 2004, Los Angeles, USA.
- [6] U. K. Müller, J. Smit, E. J. Stamhuis, J. J. Videler “How the body contributes to the wake in undulatory fish swimming: flow fields of a swimming eel (*anguilla anguilla*),” the Journal of Experimental Biology 204, 2751–2762 (2001).
- [7] J. J. Videler, E. J. Stamhuis, U. K. Mülle, L. A. Van Duren, “The Scaling and Structure of Aquatic Animal Wakes,” Integrative and Comparative Biology, Volume 42, Number 5, Pp. 988-996.
- [8] T. McMillen and P. Holmes, “An elastic rod model for anguilliform swimming,” In review, J. Math. Biol. [preprint from: <http://mae.princeton.edu/documents/McMH-swim-JMB05.pdf>]
- [9] X. Bao, Y. Bar-Cohen, S. Lih, “Measurements and Macro Models of Ionomeric Polymer-MetalComposites (IPMC),” Proc.of the SPIE Smart Structures and Materials Symposium, EAPAD Conference, San Diego, CA, March 18-21, 2002.